Journal of Nonlinear Modeling and Analysis
Volume 8, Number 2, April 2026, 338–367
http://jnma.ca; http://jnma.ijournal.cn
DOI:10.12150/jnma.2026.338

A Semi-Analytical Study on SEIR Model with Vaccinated Effects

V. Ananthaswamy[1,†], B. Sathyapriya[2] and M. Shruthi[2]

Received 18 January 2025; Accepted 16 July 2025

Abstract This research describes the dynamics of COVID-19 propagation using a mathematical model that considers vaccination and self-defence. Furthermore, the impact of vaccination on the development of disease transmission has been investigated. Our findings specifically show that putting into practice the best control measures, including time-dependent interventions, lowers the total infection load and disease transmission. Five different compartments (Susceptible, Exposed, Vaccinated, Infected, and Recovered) are used in this study to examine an epidemiological model of COVID-19 dynamics. Approximate analytical solutions to the model's system of equations were obtained using the homotopy analysis method (HAM). The numerical simulation using MATLAB was employed to validate the accuracy and effectiveness of the solutions obtained through the Homotopy Analysis Method (HAM) by comparing the results. Excellent agreement is found when comparing the approximate analytical solution and the numerical simulation. The five-compartment model includes many more aspect parameters that are explored and graphically represented. These parameters include recovery rate and vaccination rate, among others. Moreover, it underscores the potential of the HAM as a powerful tool for exploring epidemic models and formulating control strategies.

Keywords Epidemic model, COVID-19, non-linear initial value problem, Homotopy Analysis Method (HAM), numerical simulation

MSC(2010) 34A05, 34A12, 34E05, 34E10

1. Introduction

COVID-19 is a pandemic brought on by the corona virus, which began with a COVID-19 outbreak in Wuhan, China, in December 2019 [45]. The severe acute respiratory syndrome coronavirus 2 (SARS-CoV-2) was the cause of it. It started to spread early in 2020, first to Asia and then the rest of the world. After having declared the outbreak to be a public health emergency of international concern on January 30, 2020, the World Health Organization (WHO) officially declared the pandemic on March 11, 2020. A wide spectrum of symptoms, from minor symptoms to potentially fatal problems, can be caused by the COVID-19 virus. Headache, loss

[†]the corresponding author.
Email address: ananthu9777@gmail.com (V. Ananthaswamy), bspriyamaths08@gmail.com (B. Sathyapriya), mshruthi353@gmail.com (M. Shruthi).
[1]Research Centre and PG Department of Mathematics, the Madura College (Affiliated to Madurai Kamaraj University), Madurai, Tamil Nadu, India.
[2]Research Scholar, Research Centre and PG Department of Mathematics, the Madura College (Affiliated to Madurai Kamaraj University), Madurai, Tamil Nadu, India.

of taste and smell, runny nose, cough, sore throat, muscle pain, diarrhoea, high fever, and breathing difficulties are common indications and symptoms. The respiratory route is the main way in which the disease is transmitted. It happens when an infected individual exhales droplets and microscopic airborne particles that they cough, sneeze, sing, or inhale.

Precautionary steps to reduce the chance of illness consist of receiving a vaccination, remaining at home, avoiding crowded places, keeping a safe distance from other people, wearing a mask in public, washing your hands regularly for at least 20 seconds each time, practicing good respiratory hygiene, and keeping our hands clean while touching our mouth, nose, or eyes. Common mitigation tactics used during the public health emergency included quarantines, travel limitations, lockdowns, mask mandates, and contact tracking of the infected [44]. People ought to get vaccinated as soon as it is their turn. They ought to follow the vaccination recommendations made by their local authorities in order to safeguard themselves against COVID-19.

Zelenkov et al. [43] described a method that uses genetic algorithms to rebuild real transition rate distributions. This allows one to build a model that can describe multiple COVID pandemic peaks. In order to combine data-centric and analytical approaches, a model combining variant-aware compartmental models and machine learning was developed by Baccega et al. [5]. Furthermore, it unveiled a state-of-the-art system for ongoing forecasting and monitoring that fluidly combines compartmental models with predictive models based on machine learning. Gatto et al. [15] proposed an alternate hybrid strategy based on machine learning to address this issue, which omits the need to recalculate hyperparameters and just employs the initial set. Using sensitivity research, Rahman et al. [34] used the partial rank correlation coefficient technique to identify the most important components. The endemic equilibrium conditions and local asymptotic stability of the suggested COVID-19 model were demonstrated by Batistela et al. [6].

The compartmental model, which is expressed by a system of seven ODEs, is one of the new findings. Additional discoveries include numerical simulations by Lemos-Paiao et al. [23] employing real data from the Portuguese health authorities, evidence of positivity and boundedness of solutions, examination of equilibrium points and their stability analysis, and so forth. The utilization of the Monte Carlo method with Bayesian sequential design for particle filtering, as demonstrated by Li et al. [24], enables the model to be regenerated every day and to adjust to novel patterns in the daily incoming data.

Ramezani et al. [35] examined the accuracy level of our model by testing it against publicly available cumulative infection and mortality data for several US states. The findings of this study provide new light on the herd immunity and reproduction rate that is now prevalent in the US. Furthermore, the average COVID-19 reproduction number in the US was found to be 12.6 days; this puts the virus in the same category as measles and mumps as one of the most contagious diseases. A spectral technique was presented by Olivares et al. [33] that enables a polynomial extension of the stochastic state variables of the optimal control model to express the uncertainty propagation through the state variables. For compartmental epidemiological models, this method is used to create and resolve robust optimum control problems. More precisely, a polynomial chaotic expansion based on statistical moments was utilized.

Deng's [11] explanation of transmission parameters for current compartmental

models requires stochastic parameterization. Extensive data on gearbox properties is necessary for these models to function effectively. Deep learning methods work well as an alternative since they significantly lessen the reliance on data particularity when estimating these stochastic parameters. Romano et al. [37] created a deterministic compartment framework in order to perform a retrospective study and comprehend the primary alterations made to the defining qualities that control the epidemic's progression.The well-established SIR model for epidemic dynamics, the precisely known solution of linear differential equations, and the statistical method previously created for the examination of the pediatric illness that originated in Chernivtsi, Ukraine, in 1988–1989 were all utilized in the work by Nesteruk [29]. Shah et al. [40] used the Jacobian matrix to determine the local stability and fundamental reproduction number. The global stability of the problem under study was computed using the Lyapunov function theory. A numerical interpretation under fractional derivative was also attempted to be obtained by employing a fractional order non-standard finite difference (NSFD) technique. When a class of explicit 2-stage Runge-Kutta (RK2) methods of order two was applied to the numerical solution of specific non-linear initial value problems (IVPs) for ODEs on COVID-19, Khalsaraei [21] examined the positivity property for the method.

Kahn et al. [18] and colleagues employed a stochastic agent-based nursing home's susceptible-exposed-infectious (asymptomatic/symptomatic)-recovered model to imitate the spread of SARS-CoV-2. Mondal et al. [27] examined the model's qualitative behaviour and the stability of physiologically plausible equilibrium points in terms of the basic reproduction number. Hussain et al. [17] used stochastic mathematical modelling to simulate the infectious disease pandemic. Using Ito's formula, constructing suitable Lyapunov functions, and analyzing the surrounding white noise, a few subjective features are obtained. Kottakkaran Sooppy Nisar et al. [31] employed an efficient numerical method to solve the model and simulations, established existence criteria using the Banach contraction principle, and determined the reproductive number under specific state conditions. Kottakkaran Sooppy Nisar et al. [32] developed a nonlinear fractional-order Ebola model with eight compartments using a novel piecewise hybrid technique. The existence and uniqueness of solutions were established using Arzelà-Ascoli and Schauder conditions. Sensitivity analysis was performed to assess the influence of parameters on disease spread. Local and global stability were analyzed using the Matignon method and Lyapunov functions, respectively. Numerical solutions were obtained using Newton's polynomial technique for a piecewise Caputo operator, supported by real data simulations at various fractional orders.

Muhammad Umer Saleem et al. [38] developed a syphilis epidemic model using a hybrid approach combining Atangana-Baleanu Caputo and classical derivatives to capture memory effects across different time phases. Generalized Ulam-Hyers stability ensured global stability, and the piecewise model was shown to have a unique solution. Numerical solutions were obtained using Newton polynomial interpolation for various fractional orders. Sant Ram Chawla et al. [9] used LaSalle's invariance principle and Lyapunov's direct method to show that less than 1 ensures global asymptotic stability of the disease-free equilibrium. Optimal control strategies were determined using Pontryagin's Maximum Principle. Naik et al. [28] developed a time-fractional COVID-19 model using a generalized Mittag-Leffler kernel and a fractal-fractional operator to capture infection rate fluctuations. Existence, uniqueness, and Ulam-Hyers stability were established using the Banach

contraction principle.

By constructing a suitable stochastic Lyapunov functional, Bera et al. [7] analyzed the qualitative properties of the stochastic HTLV-I infection model, including the existence and uniqueness of solutions, stochastic ultimate boundedness, and uniform continuity. The proposed system exhibits three biologically feasible steady states: the disease-free steady state, the CTL-inactive steady state, and the interior steady state. Bera et al. [8] estimated the critical time delay that preserves the stability of the period-1 limit cycle. The direction and stability of the Hopf bifurcation near the interior steady state were analyzed using center manifold theory and the normal form method. To assess the robustness of the model, a normalized forward sensitivity analysis was performed with respect to R0 and R1. Das et al. [10] proposed and analyzed a mathematical model for tuberculosis transmission that incorporates the impact of social awareness during an epidemic. The model's possible equilibrium points were identified, and their stability criteria were examined. The basic reproduction number was derived using the next-generation matrix method.

Dwivedi et al. [12] analyzed a nonlinear vector-host dengue model with vaccination and treatment controls, calibrated using data from six Indian states. Sensitivity analysis showed that reducing transmission rates between mosquitoes and humans is key to controlling the disease. Khajanchi et al. [20] carried out a sensitivity analysis to identify the key parameters of the HTLV-I infection model with respect to the reproduction number. Tiwari et al. [41] conducted a sensitivity analysis to identify the key parameters of the model that have significant impacts on the prevalence and control of COVID-19. Ghosh et al. [16] analyzed a model with two equilibrium points—disease-free and interior—examining positivity, boundedness, and global stability. The basic reproduction number was derived using the next-generation matrix method. Khajanchi et al. [19] examined the dynamical behavior of the system both analytically and numerically from the perspectives of stability and optimal control theory. In the case of non-constant control, Pontryagin's Maximum Principle was applied to derive the necessary conditions for an optimal control strategy for HTLV-I infection.

Atangana [3] employed a study of the Lyapunov functions second derivative in addition to an investigation of each class second derivative to determine how a wave may be identified. Additionally, the proposed model's stochastic variant was examined. The next generation matrix was used by Atangana [2] to implement a lockdown and social distancing effect. Atangana et al. [4] provided a full presentation of the reproduction number formula and the stability analysis for the novel mathematical model COVID-19, which was composed of nine classes. Utilizing the Atangana-Baleanu in the Caputo sense fractional derivative, Xu et al. [42] examined the fractional-order COVID-19 model. Farmant et al. [14] used the Sumudu transform (ST) approach in their investigation of the fractional-order COVID-19 model.

Our motivation to solve the problem and provide approximate analytical solutions came from the aforementioned studies. Evaluating the semi-analytical solution for the COVID-19 epidemiology using HAM is the main objective of this research. When the results obtained from the Homotopy Analysis Method (HAM) are compared with other numerical solutions, they provide explicit expressions that are highly valuable for evaluating the epidemic model of disease transmission and understanding the influence of various parameters. While HAM does not guarantee approximate analytical solutions for all first-order nonlinear initial value problems,

it has been effectively applied in our study to solve the first-order nonlinear model of COVID-19 and to derive explicit semi-analytical expressions. The numerical simulation and approximate analytical solution are then shown in a comparison and graphical format. To illustrate the impact of multiple variables, graphical representations are presented.

Nomenclature:

Symbol	Meaning
ρ_1	Contact rate
μ_0	Death rate due to infection
$I(t)$	Infected
a	Recruitment rate
ω	Rate at which an individual becomes recovered
$E(t)$	Exposed
α	Rate at which the infection is reducing due to vaccination
ρ_2	Vaccination rate
$R(t)$	Recovered
b	Recruitment rate to the vaccinated class
$S(t)$	Susceptible
t	Time (days)
$V(t)$	Vaccinated
ψ	Recovery rate
δ	Death rate due to natural causes
ϕ	Contact rate from the vaccinated to the infected class
ρ	Migration rate from the susceptible to exposed
$N(t)$	Total population

2. Mathematical formulation of the problem

Let's examine the SARS-COVID-19 model as presented by Huda Alsaud et al. [1] in which the classes S stands for susceptible, E for exposed, V for vaccinated, I for infected and R for recovered. We specify a number of parameters for this model: a is the recruitment rate, δ is the percentage of deaths from natural causes, the rate of interaction between the vulnerable and exposed classes is represented by $\rho + \rho_1$, ρ_2 is the vaccination rate, the rate of infection reduction as a result of vaccination effects is symbolized by α, μ_0 is the infection-related mortality rate, ω is a measure of how quickly a person recovers from a vaccination and gets well, b is a representation of the vaccination class enrollment rate, the proportion of contact between the immunized and infected groups is represented by ϕ and ψ is

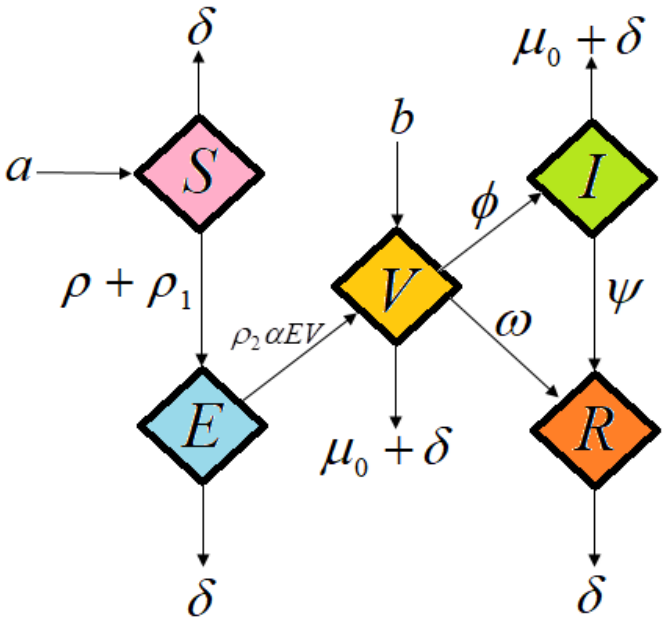

Figure 1. Diagrammatic depiction of the pandemic model

the recovery rate. Our goal is to investigate how the vaccine impact spreads the SARS-COVID-19.

The following is the framework that was created using the vaccine effect as the basis for the generalized hypothesis:

$$\frac{dS}{dt} = a - (\delta + \rho + \rho_1)S, \tag{2.1}$$

$$\frac{dE}{dt} = (\rho + \rho_1)S - \delta E - \rho_2 \alpha EV, \tag{2.2}$$

$$\frac{dV}{dt} = \rho_2 \alpha EV - (\delta + \mu_0 + \omega - b + \phi)V, \tag{2.3}$$

$$\frac{dI}{dt} = \phi V - (\mu_0 + \delta + \psi)I, \tag{2.4}$$

$$\frac{dR}{dt} = \omega V + \psi I - \delta R \tag{2.5}$$

with initial condition

$$At\ t = 0, S(0) = c_1 > 0, E(0) = c_2 > 0, V(0) = c_3 > 0, I(0) = c_4 > 0, R(0) = c_5 > 0. \tag{2.6}$$

The model schematic diagram is depicted in Figure 1. A brief description of the compartments and transitions in Fig 1 is provided below:

• Susceptible: Becomes exposed at rate $\rho + \rho_1$, and exits the system at rate δ. New susceptible enter at rate a.

• Exposed: Transitions to vaccinated V at rate $\rho_2 \alpha EV$, and exits at rate δ.

• Vaccinated: Receives people from E, moves to infectious I at rate b, or to recovered

R at rate ω. Leaves the system at $\mu_0 + \delta$.
• Infected: Infected individuals may recover at rate ϕ, or exit at $\mu_0 + \delta$.
• Recovered: Gains from I and V, and exits at δ.

3. Approximate analytical solutions for the SEVIR model using the Homotopy Analysis Method

Laplace adomain decomposition procedure [13], Homotopy analysis approach [36], Homotopy perturbation technique [22], and the new approach to Homotopy perturbation strategy [39] are asymptotic methods used to derive approximate analytic solutions to non-linear differential equations. The Homotopy Analysis Method (HAM) is a non-perturbative analytical technique that has been successfully applied across a wide range of scientific and engineering problems. It operates by constructing series solutions to nonlinear differential equations. A key feature of HAM is the convergence-control parameter, which allows flexibility in ensuring and adjusting the convergence of the solution. Consequently, HAM has proven to be a highly effective method for obtaining analytical solutions to nonlinear differential equations. In most cases, HAM addresses nonlinearity by representing the unknown function and its derivatives as a polynomial. The HAM yields a simpler, more accurate solution than any of these other approaches. Liao [25, 26] introduced the homotopy analysis approach, a potent analytical technique for non-linear situations. This method's benefit is that it only requires one convergence control parameter within the system, making it suitable for a variety of solutions of non-linear differential equations.

Eqns.(2.1)-(2.6) can have their homotopy using HAM as follows.

$$(1-p)\left[\frac{dS}{dt} + (\delta+\rho+\rho_1)S\right] = hp\left[\frac{dS}{dt} - a + (\delta+\rho+\rho_1)S\right], \tag{3.1}$$

$$(1-p)\left[\frac{dE}{dt} + \delta E\right] = hp\left[\frac{dE}{dt} - (\rho+\rho_1)S + \delta E + \rho_2\alpha EV\right], \tag{3.2}$$

$$(1-p)\left[\frac{dV}{dt} + (\delta+\mu_0+\omega-b+\phi)V\right] = hp\left[\frac{dV}{dt} - \rho_2\alpha EV + (\delta+\mu_0+\omega-b+\phi)V\right], \tag{3.3}$$

$$(1-p)\left[\frac{dI}{dt} + (\mu_0+\delta+\psi)I\right] = hp\left[\frac{dI}{dt} - \phi V + (\mu_0+\delta+\psi)I\right], \tag{3.4}$$

$$(1-p)\left[\frac{dR}{dt} + \delta R\right] = hp\left[\frac{dR}{dt} - \omega V - \psi I + \delta R\right]. \tag{3.5}$$

The approximate analytical solution to Eqns.(3.1)-(3.5) is as follows:

$$S = S_0 + pS_1 + p^2S_2 + ..., \tag{3.6}$$

$$E = E_0 + pE_1 + p^2E_2 + ..., \tag{3.7}$$

$$V = V_0 + pV_1 + p^2V_2 + ..., \tag{3.8}$$

$$I = I_0 + pI_1 + p^2I_2 + ..., \tag{3.9}$$

$$R = R_0 + pR_1 + p^2R_2 + ... \tag{3.10}$$

For Eqns.(3.1) to (3.5), the initial approximations are given by

$$S_0(0) = c_1,\ \ E_0(0) = c_2,\ \ V_0(0) = c_3,\ \ I_0(0) = c_4, R_0(0) = c_5, \tag{3.11}$$
$$S_i(0) = 0,\ \ E_i(0) = 0,\ \ V_i(0) = 0,\ \ I_i(0) = 0, R_i(0) = 0, i = 1, 2, 3, ... \tag{3.12}$$

We have to put Eqns.(3.6)-(3.10) into Eqns.(3.1)-(3.5) and compare the coefficients of the powers of p^0 and p^1 so as to arrive at the following equations.
Zeroth iterations:

$$p^0 : \frac{dS_0}{dt} + (\delta + \rho + \rho_1)S_0 = 0, \tag{3.13}$$
$$p^0 : \frac{dE_0}{dt} + (\delta)E_0 = 0, \tag{3.14}$$
$$p^0 : \frac{dV_0}{dt} + (\delta + \mu_0 + \omega - b + \phi)V_0 = 0, \tag{3.15}$$
$$p^0 : \frac{dI_0}{dt} + (\mu_0 + \delta + \psi)I_0 = 0, \tag{3.16}$$
$$p^0 : \frac{dR_0}{dt} + \delta R_0 = 0. \tag{3.17}$$

Initial iterations:

$$p^1 : \frac{dS_1}{dt} + (\delta + \rho + \rho_1)S_1 - \frac{dS_0}{dt} - (\delta + \rho + \rho_1)S_0 - h\left(\frac{dS_0}{dt} - a + (\delta + \rho + \rho_1)S_0\right) = 0, \tag{3.18}$$
$$p^1 : \frac{dE_1}{dt} + (\delta)E_1 - \frac{dE_0}{dt} - (\delta)E_0 - h\left(\frac{dE_0}{dt} - (\rho + \rho_1)S_0 + \delta E_0 + \rho_2\alpha E_0 V_0\right) = 0, \tag{3.19}$$
$$p^1 : \frac{dV_1}{dt} + (\delta + \mu_0 + \omega - b + \phi)V_1 - \frac{dV_0}{dt} - (\delta + \mu_0 + \omega - b + \phi)V_0, - h\left(\frac{dV_0}{dt} - \rho_2\alpha E_0 V_0 + (\delta + \mu_0 + \omega - b + \phi)V_0\right) = 0, \tag{3.20}$$
$$p^1 : \frac{dI_1}{dt} + (\mu_0 + \delta + \psi)I_1 - \frac{dI_0}{dt} - (\mu_0 + \delta + \psi)I_0 - h\left(\frac{dI_0}{dt} - \phi V_0 + (\mu_0 + \delta + \psi)I_0\right) = 0, \tag{3.21}$$
$$p^1 : \frac{dR_1}{dt} + \delta R_1 - \frac{dR_0}{dt} - \delta R_0 - h\left(\frac{dR_0}{dt} - \omega V_0 - \psi I_0 + \delta R_0\right) = 0. \tag{3.22}$$

We can obtain the following results by solving Eqns.(3.13)-(3.17) using the constraints in Eqns. (3.11):

$$S_0 = c_1\ e^{-(\delta+\rho+\rho_1)\,t}, \tag{3.23}$$
$$E_0 = c_2\ e^{-(\delta)\,t}, \tag{3.24}$$
$$V_0 = c_3\ e^{-(\delta+\mu_0+\omega-b+\phi)\,t}, \tag{3.25}$$
$$I_0 = c_4\ e^{-(\mu_0+\delta+\psi)\,t}, \tag{3.26}$$
$$R_0 = c_5\ e^{-(\delta)\,t}. \tag{3.27}$$

We can obtain the following results by solving Eqns.(3.13)-(3.17) and (3.18)-(3.22) using the constraints (3.11) and (3.12)

$$S_1 = \frac{h\,a\ e^{-(\delta+\rho+\rho_1)\,t}}{\delta+\rho+\rho 1} - \frac{h\,a}{\delta+\rho+\rho_1}, \tag{3.28}$$

$$E_1 = -\frac{h\,(\rho+\rho_1)\,c_1\ e^{-(\delta)\,t}}{(\rho+\rho_1)} + \frac{h\,\rho_2\alpha c_2\,c_3\,e^{-(\delta)\,t}}{(\delta+\mu_0+\omega-b+\phi)} + \frac{h\,(\rho+\rho_1)\,c_1\ e^{-(\delta+\rho+\rho_1)\,t}}{(\rho+\rho_1)} - \frac{h\,\rho_2\alpha c_2\,c_3\,e^{-(2\delta+\mu_0+\omega-b+\phi)\,t}}{(\delta+\mu_0+\omega-b+\phi)}, \tag{3.29}$$

$$V_1 = -\frac{h\,\rho_2\alpha c_2\,c_3\,e^{-(\delta+\mu_0+\omega-b+\phi)\,t}}{\delta} + \frac{h\,\rho_2\alpha c_2\,c_3\,e^{-(2\delta+\mu_0+\omega-b+\phi)\,t}}{\delta}, \tag{3.30}$$

$$I_1 = \frac{h\,\phi\,c_3\ e^{-(\mu_0+\delta+\psi)\,t}}{\psi-\omega+b-\phi} - \frac{h\,\phi\,c_3\ e^{-(\delta+\mu_0+\omega-b+\phi)\,t}}{\psi-\omega+b-\phi}, \tag{3.31}$$

$$R_1 = \frac{h\,\omega\,c_3\ e^{-(\delta)\,t}}{b-\mu_0-\omega-\phi} - \frac{h\,\psi\,c_4\ e^{-(\delta)\,t}}{\mu_0+\psi} - \frac{h\,\omega\,c_3\ e^{-(\delta+\mu_0+\omega-b+\phi)\,t}}{b-\mu_0-\omega-\phi} + \frac{h\,\psi\,c_4\ e^{-(\delta+\mu_0+\psi)\,t}}{\mu_0+\psi}. \tag{3.32}$$

According to HAM technique, we have

$$S = \lim_{p\to 1} S(t) = S_0 + S_1, \tag{3.33}$$

$$E = \lim_{p\to 1} E(t) = E_0 + E_1, \tag{3.34}$$

$$V = \lim_{p\to 1} V(t) = V_0 + V_1, \tag{3.35}$$

$$I = \lim_{p\to 1} I(t) = I_0 + I_1, \tag{3.36}$$

$$R = \lim_{p\to 1} R(t) = R_0 + R_1. \tag{3.37}$$

As a result, by substituting the Eqns.(3.23) to (3.32) into Eqns.(3.33) to (3.37), we have the following approximate analytical solutions.

$$S(t) = c_1\ e^{-(\delta+\rho+\rho_1)\,t} + \frac{h\,a\ e^{-(\delta+\rho+\rho_1)\,t}}{\delta+\rho+\rho_1} - \frac{h\,a}{\delta+\rho+\rho_1}, \tag{3.38}$$

$$E(t) = c_2\ e^{-\delta\,t} - \frac{h\,(\rho+\rho_1)\,c_1\ e^{-\delta\,t}}{(\rho+\rho_1)} + \frac{h\,\rho_2\alpha c_2\,c_3\,e^{-\delta\,t}}{(\delta+\mu_0+\omega-b+\phi)} + \frac{h\,(\rho+\rho_1)\,c_1\ e^{-(\delta+\rho+\rho_1)\,t}}{(\rho+\rho_1)} - \frac{h\,\rho_2\alpha c_2\,c_3\,e^{-(2\delta+\mu_0+\omega-b+\phi)\,t}}{(\delta+\mu_0+\omega-b+\phi)}, \tag{3.39}$$

$$V(t) = c_3\ e^{-(\delta+\mu_0+\omega-b+\phi)\,t} - \frac{h\,\rho_2\alpha c_2\,c_3\,e^{-(\delta+\mu_0+\omega-b+\phi)\,t}}{\delta} + \frac{h\,\rho_2\alpha c_2\,c_3\,e^{-(2\delta+\mu_0+\omega-b+\phi)\,t}}{\delta}, \tag{3.40}$$

$$I(t) = c_4\ e^{-(\mu_0+\delta+\psi)\,t} + \frac{h\,\phi\,c_3\ e^{-(\mu_0+\delta+\psi)\,t}}{\psi-\omega+b-\phi} - \frac{h\,\phi\,c_3\ e^{-(\delta+\mu_0+\omega-b+\phi)\,t}}{\psi-\omega+b-\phi}, \tag{3.41}$$

$$R(t) = c_5\ e^{-\delta\,t} + \frac{h\,\omega\,c_3\ e^{-\delta\,t}}{b-\mu_0-\omega-\phi} - \frac{h\,\psi\,c_4\ e^{-\delta\,t}}{\mu_0+\psi} - \frac{h\,\omega\,c_3\ e^{-(\delta+\mu_0+\omega-b+\phi)\,t}}{b-\mu_0-\omega-\phi}$$

$$+\frac{h\,\psi\,c_4\;e^{-(\delta+\mu_0+\psi)\,t}}{\mu_0+\psi}. \tag{3.42}$$

4. Numerical simulation

Numerical simulation of non-linear differential equations demonstrates the efficacy of our approximate-analytical solution. In MATLAB, the function graphmain 3 is used for Eqns.(2.1) to (2.6). Figs.2–7 demonstrate the good agreement between our approximate-analytical solution and the numerical simulation.

5. Results and discussion

This section has covered the graphical representation using the approximate analytical results listed in Eqns.(3.38) to (3.42). Figures 2 to 29 show a comparison between the approximate analytical results and numerical simulation. The following describes how disease spread behaves under control intervention. ρ_1 determines the frequency of contact between susceptible people and sick people, which aids in the spread of the disease, μ_0 represents additional disease-related mortality in the infected compartment beyond the natural death rate, a characterizes the influx of new people into the vulnerable population, such as births or immigration, ω shows the rate at which infected people recover and enter the recovered class, α represents the efficiency of vaccination in lowering the rate of transmission, ρ_2 regulates the rate at which vulnerable people receive vaccinations and join the immunized group, b refers to new people who join the vaccinated population directly, whether through births or other means. When people recover from an infection, ψ stands for a general recovery parameter, δ is the standard mortality rate that applies to every compartment, ϕ suggests breakthrough infections or partial immunity by simulating possible transmission among vaccinated individuals and ρ reflects the migration of populations.

Fig.2: Depicts the population as a whole over time for the epidemic model under consideration. The susceptible, exposed, infected, vaccinated, and recovered classes of population are plotted versus time for a few model-fixed parameters in this figure.

For Susceptible class: Using Eqn.(3.38), the susceptible class $S(t)$ is displayed against time (t) (days) in Figs.3–6. The values of the Recruitment rate a grow in parallel with an increase in the corresponding susceptible class $S(t)$, as shown in Figure 3. The corresponding Susceptible class $S(t)$ decreases as the amount of deaths from natural causes δ, the migration rate from Susceptible to Exposed ρ, and the contact rate ρ_1 increase, as shown in Figures 4, 5, and 6.

For Exposed class: Figs.7–11 show the exposed class $E(t)$ versus time (t) with the use of Eqn.(3.39). Figs.7 and 8 show that an increase in the contact rate and migration rate from Susceptible to Exposed ρ causes an equal increase in the Exposed class. The matched Exposed class $E(t)$ experiences declining rates, whereas the vaccination rate ρ_2 , the pace at which the infection is decreasing as a result of vaccination α, and the mortality rate from natural causes δ all show rising values. Figures 9–11 provide illustrations of these findings.

For Vaccinated class: The Vaccinated class $V(t)$ versus time (t) is shown in Figs.12–18 using Eqn.(3.40). In accordance with Figs.12, 13, and 17, the correspond-

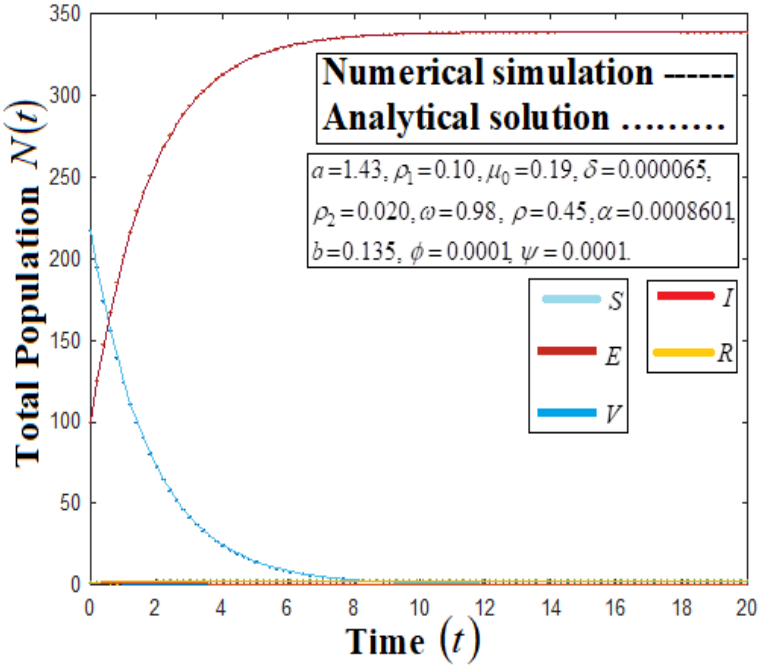

Figure 2. Total population versus time for five classes.

ing Vaccinated class $V(t)$ likewise grows when the vaccination rate ρ_2, infection rate decreasing as a result of vaccination α and recruitment rate to the vaccinated class b, increases. The corresponding Vaccinated class $V(t)$ declines, whereas the rates of infection μ_0, natural causes of death δ, the rate at which a person recovers ω, and contact rates between the vaccinated and the infected classes ϕ all show growing values. Figures 14–16 and 18 provide illustrations of these findings.

For Infected class: Figs.19–24 display the infected class $I(t)$ versus time (t) using Eqn.(3.41). The corresponding infected class $I(t)$ declines as the pace of recuperation ψ, the speed at which someone heals ω, the death rate from infection μ_0, and the death rate from natural causes δ all rise, as illustrated in Figs. 20, 21, 23, and 24. Infected Class $I(t)$ rises with an increasing rate of communication between immunized and affected class ϕ and with the recruitment rate to the vaccinated class b, as seen in Figs. 19 and 22.

For Recovered class: Eqn.(3.42) is used to plot the Recovered class $R(t)$ against time (t) in Figures 25–29. As seen in Figs. 28 and 29, the benefits of infection-related death rate μ_0, rate of interaction between the immunized and the affected group ϕ all increase, while the corresponding Recovered class $R(t)$ decreases. The increase in the rate at which a person gets recovered ω, the pace of recovery ψ, and the enrollment rate for the class of immunized individuals b and the recovered class $R(t)$ are positively correlated, as shown in Figures 25–27.

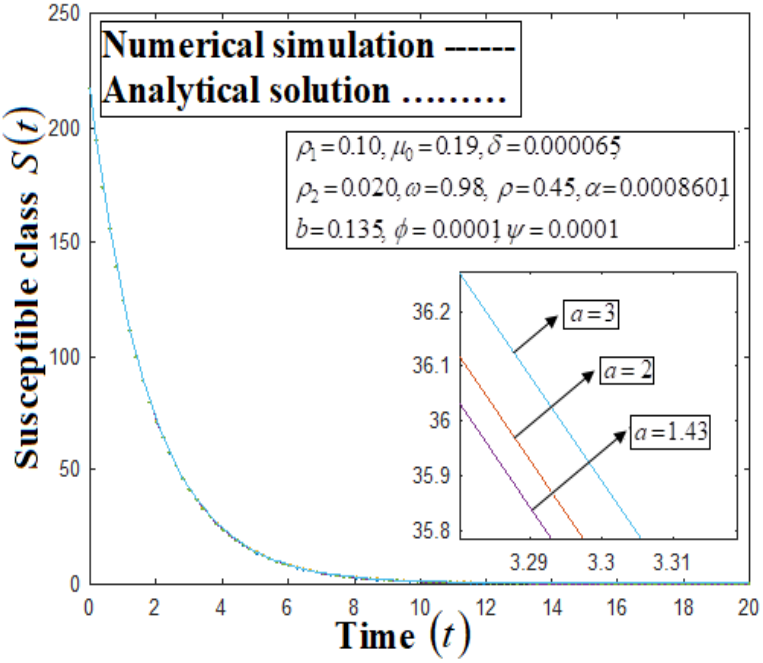

Figure 3. The impact of the recruitment rate a in susceptible $S(t)$.

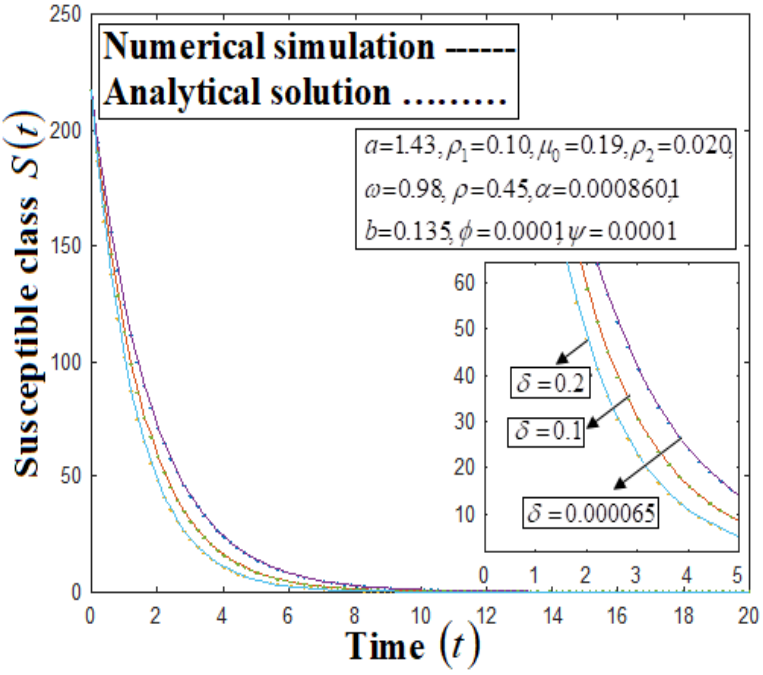

Figure 4. The influence of the death rate due to natural causes δ in susceptible $S(t)$.

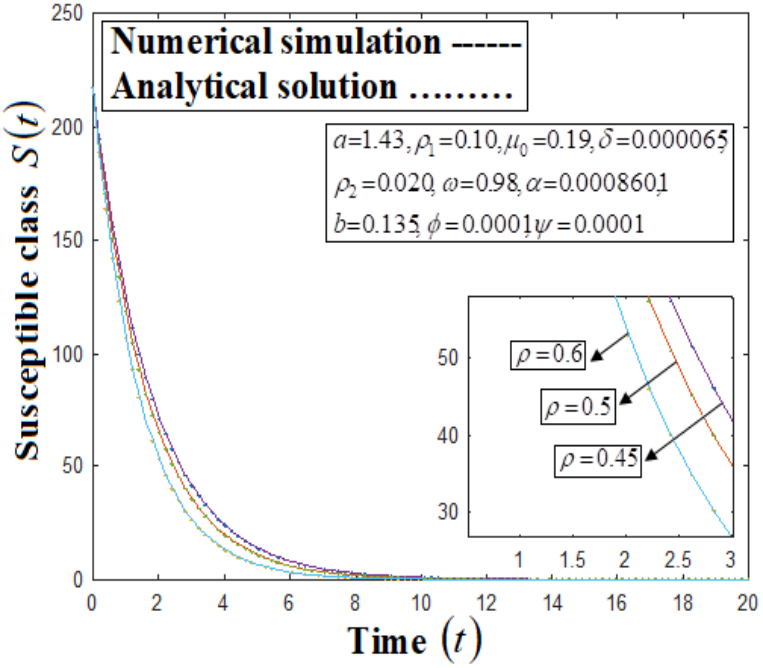

Figure 5. The effects of the migration rate from susceptible to exposed ρ in susceptible $S(t)$.

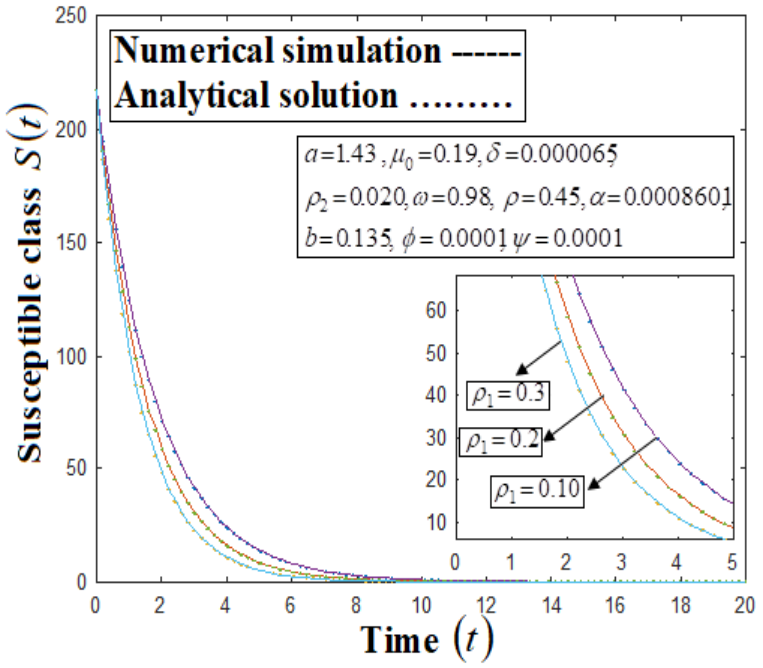

Figure 6. Variation in the contact rate ρ_1 in susceptible $S(t)$.

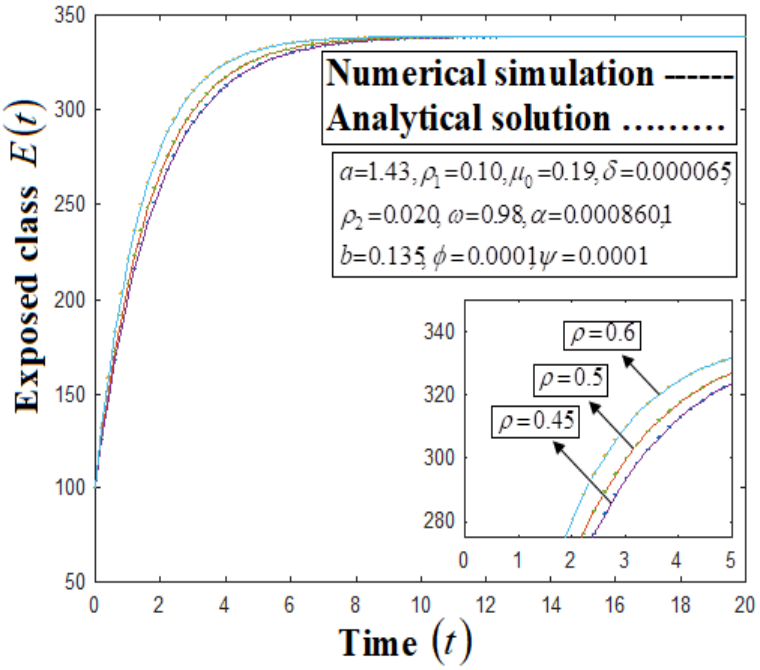

Figure 7. The effect of the migration rate from susceptible to exposed ρ in exposed $E(t)$.

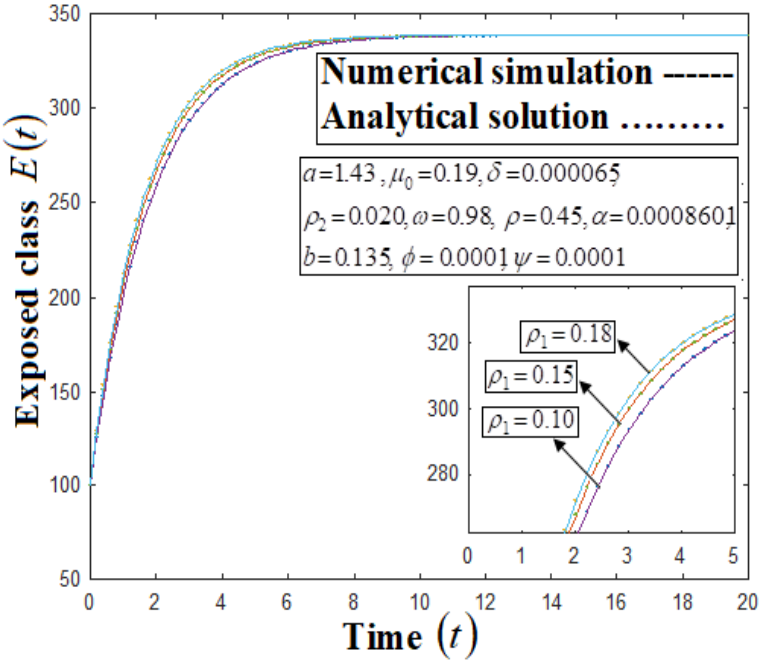

Figure 8. The effects of contact rate ρ_1 in exposed $E(t)$.

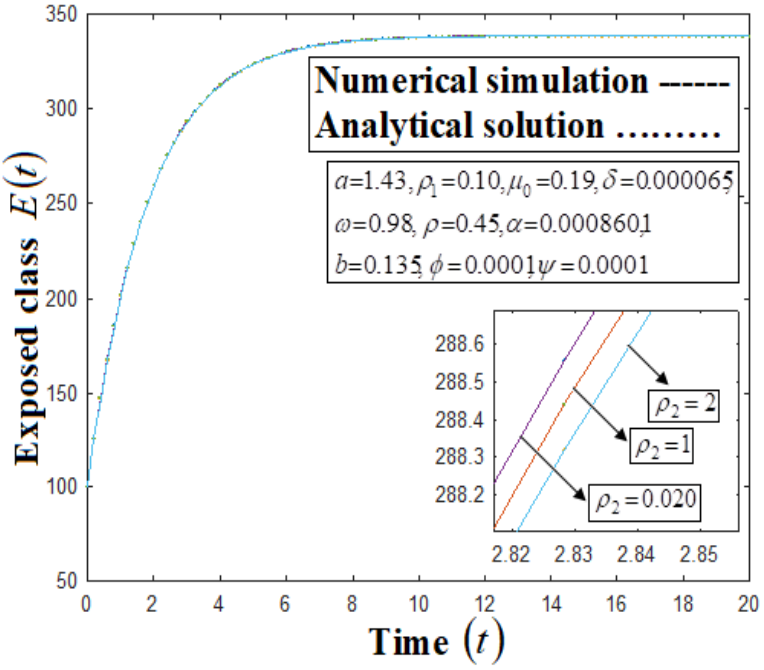

Figure 9. Results of the vaccination rate ρ_2 in exposed $E(t)$.

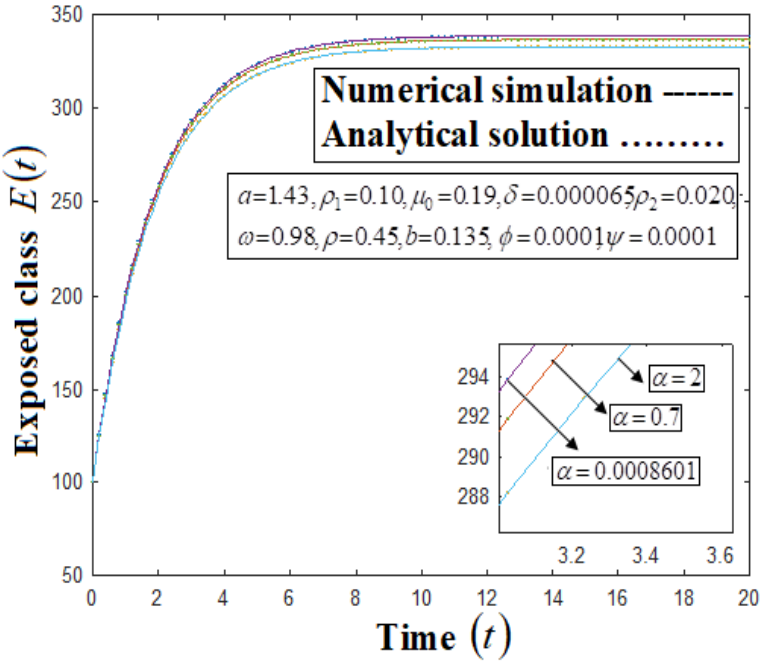

Figure 10. Significance of the speed at which vaccination is lowering infection α in exposed $E(t)$.

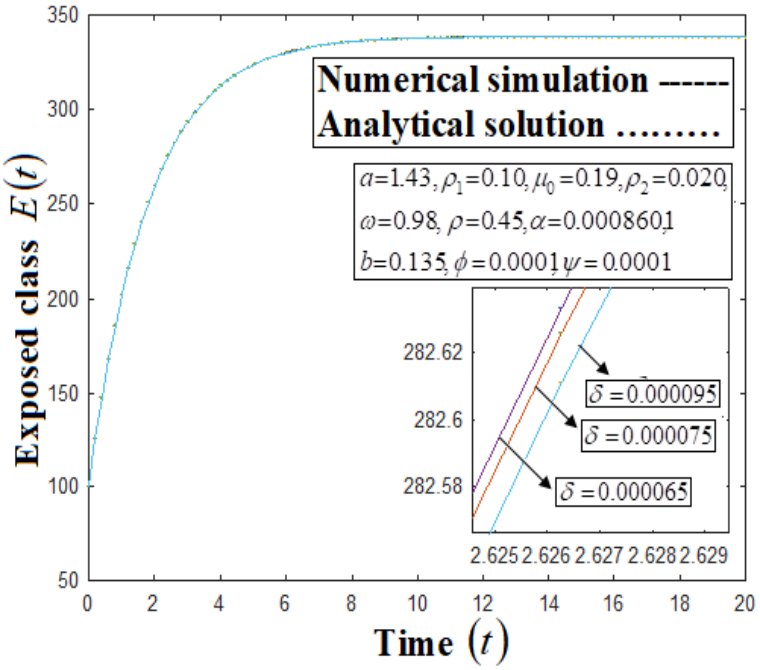

Figure 11. Variance of death rate due to natural causes δ in exposed $E(t)$.

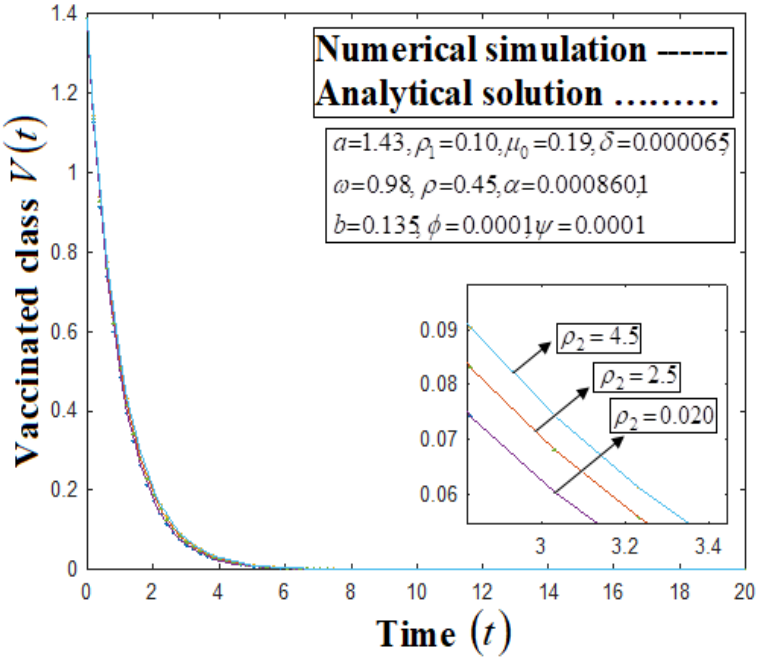

Figure 12. The consequence of vaccination rate ρ_2 in vaccinated $V(t)$.

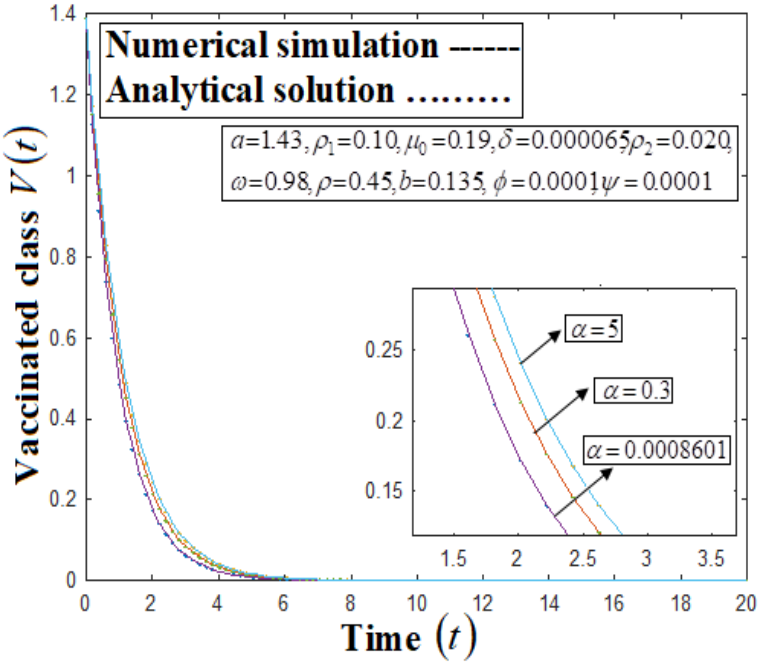

Figure 13. Significance of the pace at which immunization is decreasing infection α in vaccinated $V(t)$.

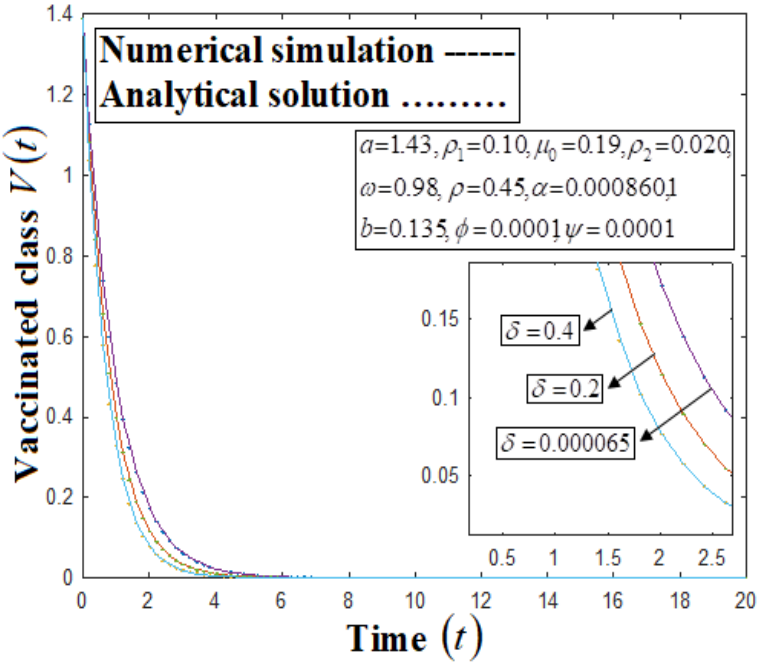

Figure 14. Effects of death rate due to natural causes δ in vaccinated $V(t)$.

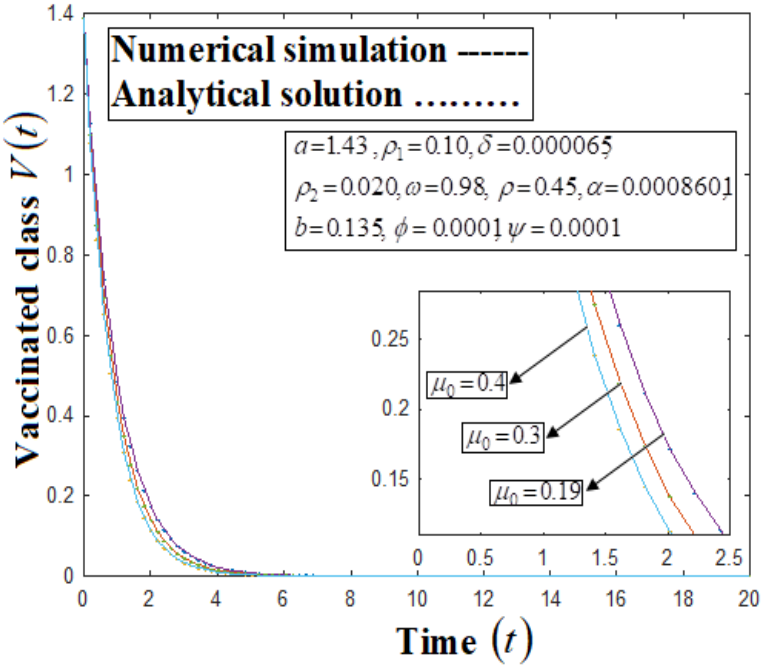

Figure 15. Variation of death rate due to infection μ_0 in vaccinated $V(t)$.

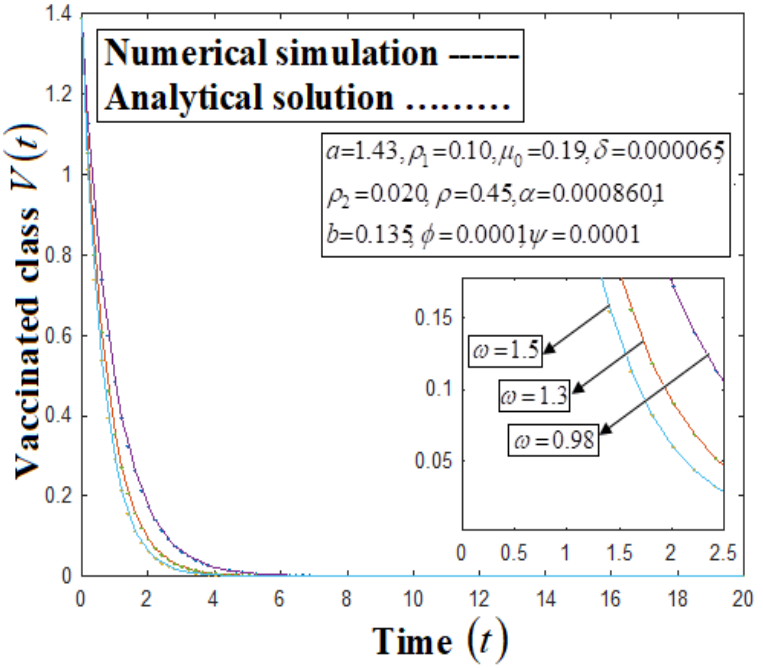

Figure 16. Consequence of which an individual's becomes recovered ω in vaccinated $V(t)$.

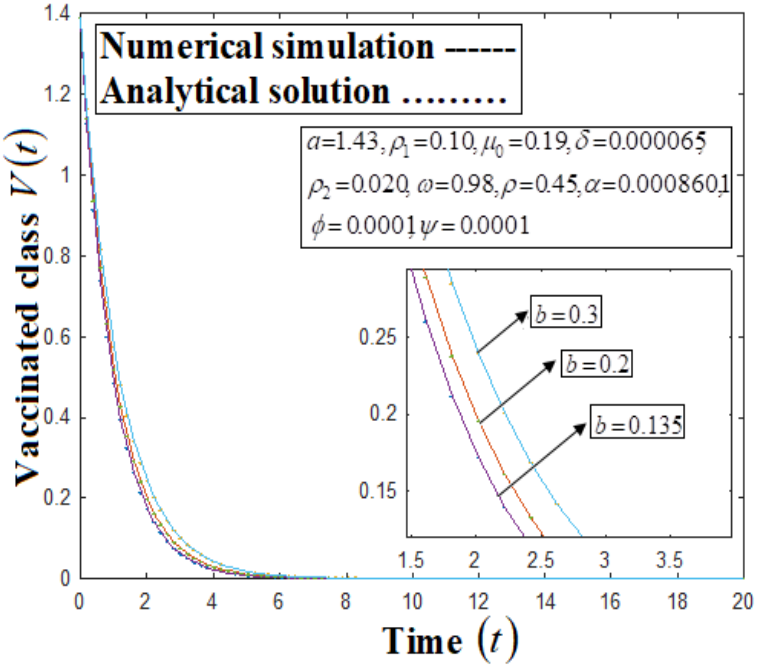

Figure 17. The impacts in recruitment rate to the vaccinated class b in vaccinated $V(t)$.

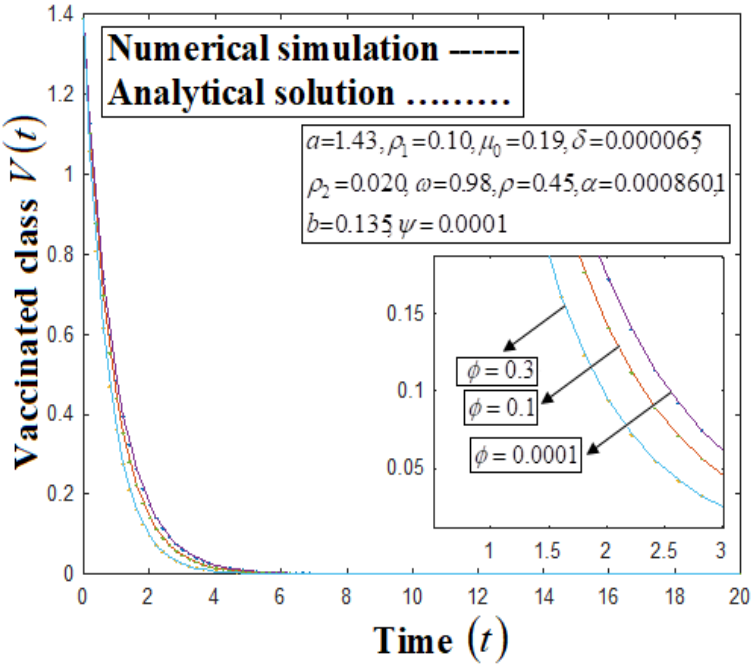

Figure 18. The influence of the percentage of contact between the immunized and diseased classes ϕ in vaccinated $V(t)$.

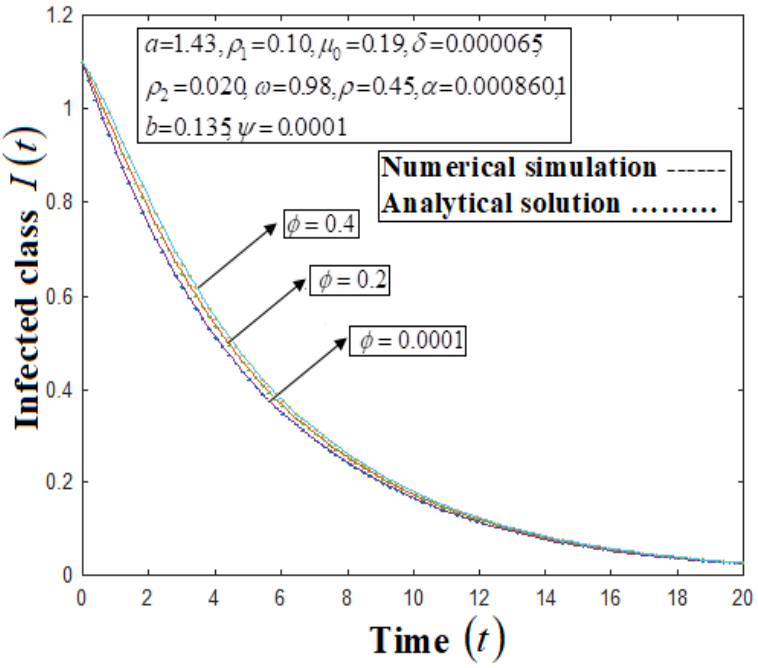

Figure 19. Variations of the percentage of vaccination-to-infected contact ϕ in infected $I(t)$.

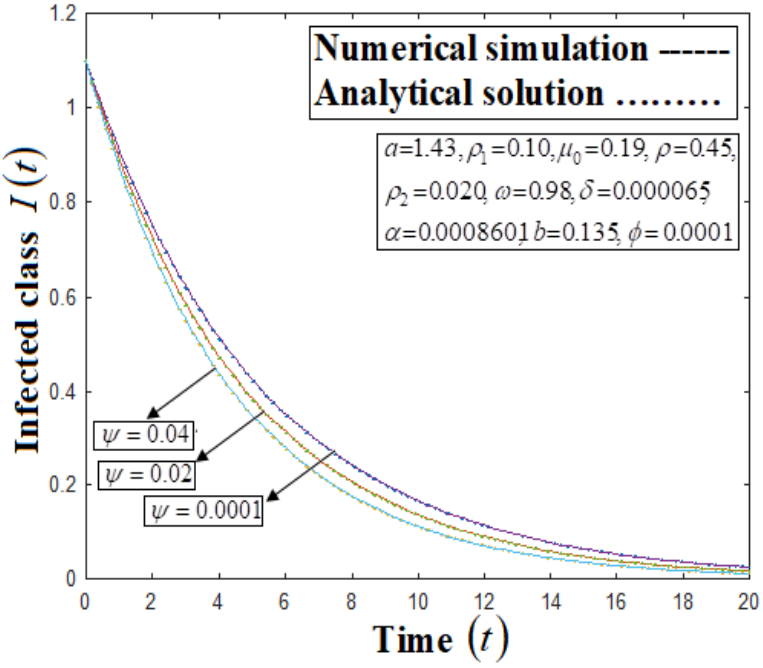

Figure 20. The influence of recovery rate ψ in infected $I(t)$.

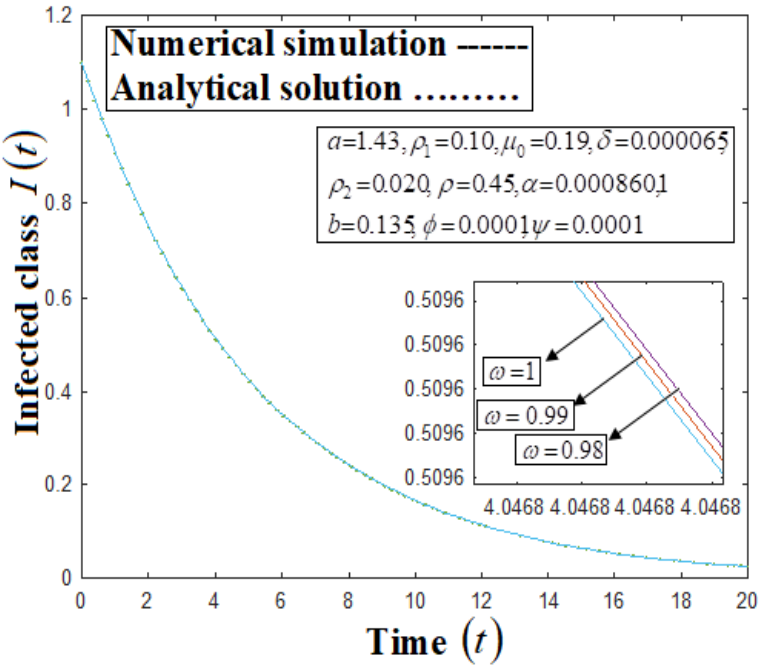

Figure 21. The implications of the rate of recovery for an individual ω in infected $I(t)$.

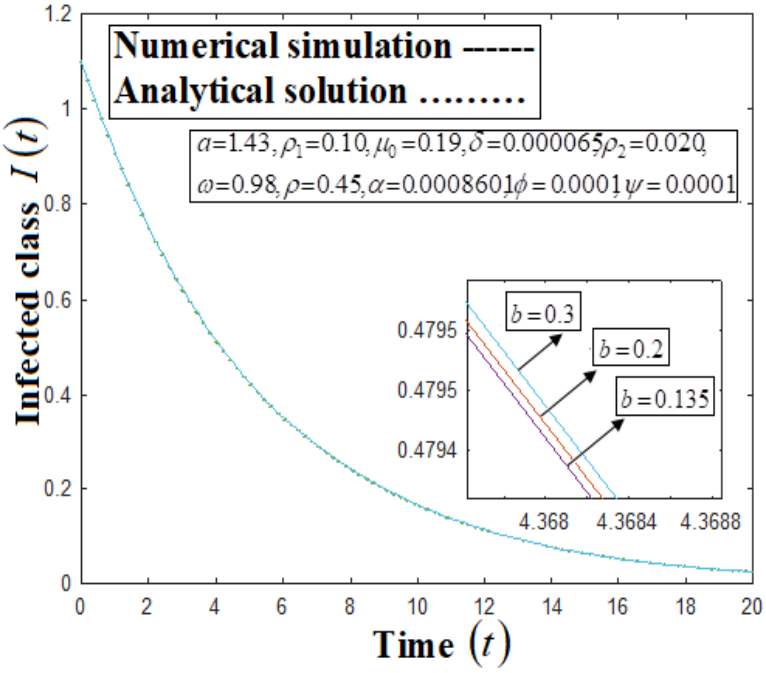

Figure 22. Variation of the enrollment percentage for the immunization class b in the infected $I(t)$.

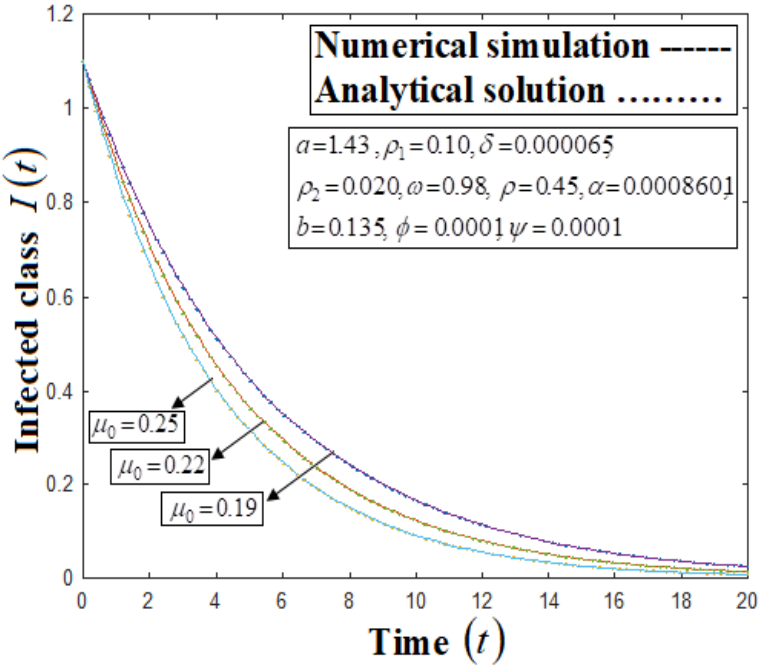

Figure 23. Impact of the mortality rate due to infection μ_0 in the infected $I(t)$.

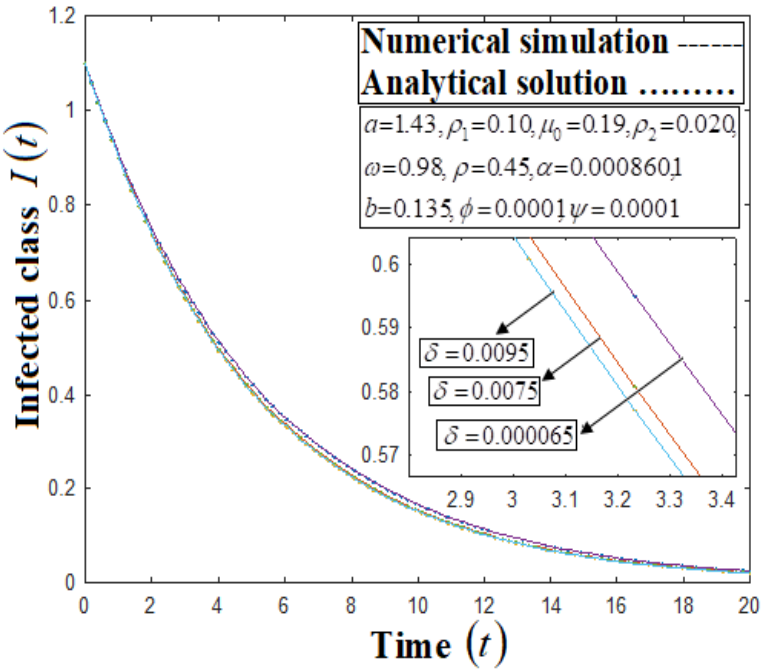

Figure 24. The impacts of the death rate due to natural reasons δ in the infected $I(t)$.

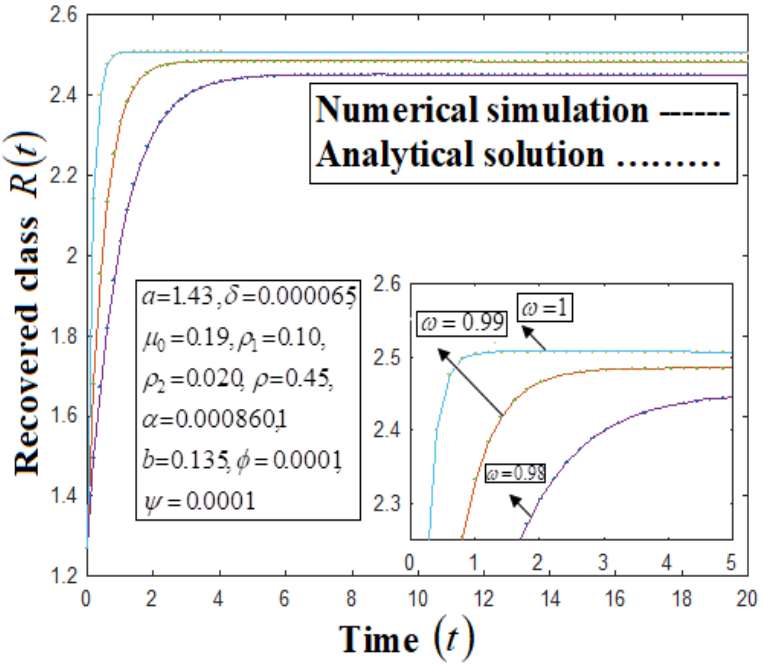

Figure 25. The influence of pace at which a person's becomes recovered ω in recovered $R(t)$.

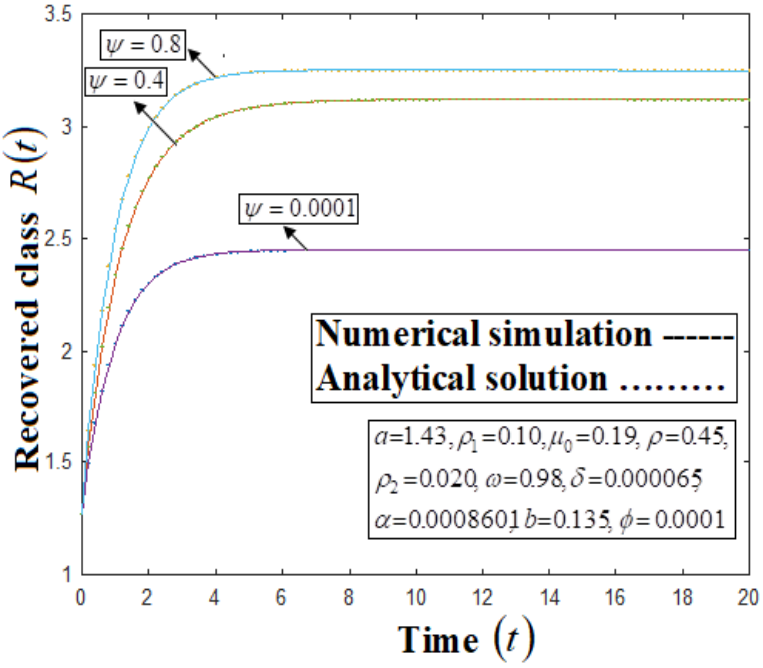

Figure 26. The recovery rate variation ψ in recovered $R(t)$.

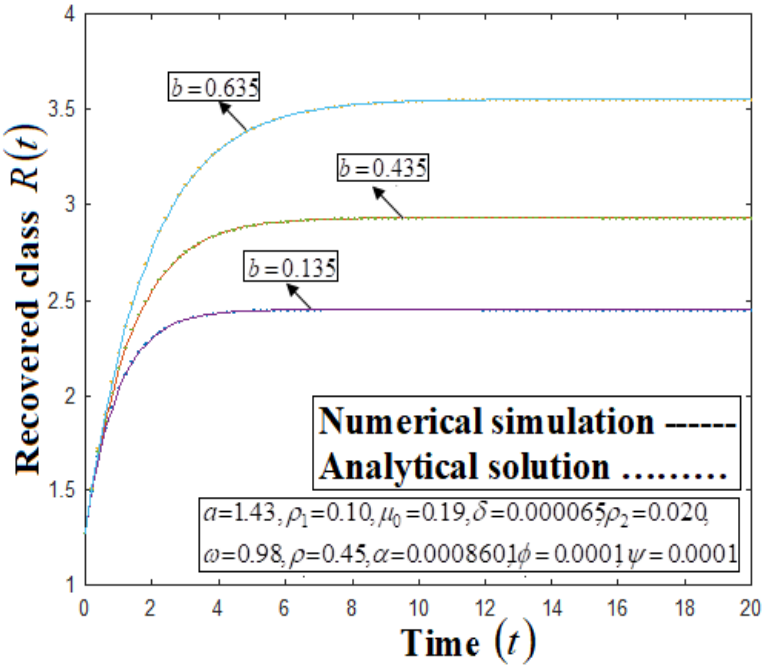

Figure 27. The implications of the vaccination class's recruitment rate b in recovered $R(t)$.

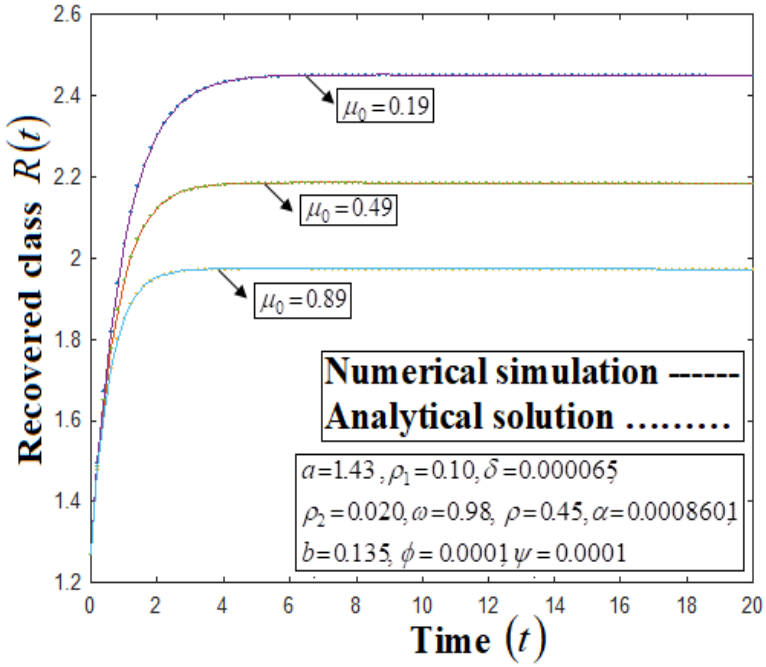

Figure 28. The implications of the infection-related mortality rate μ_0 in recovered $R(t)$.

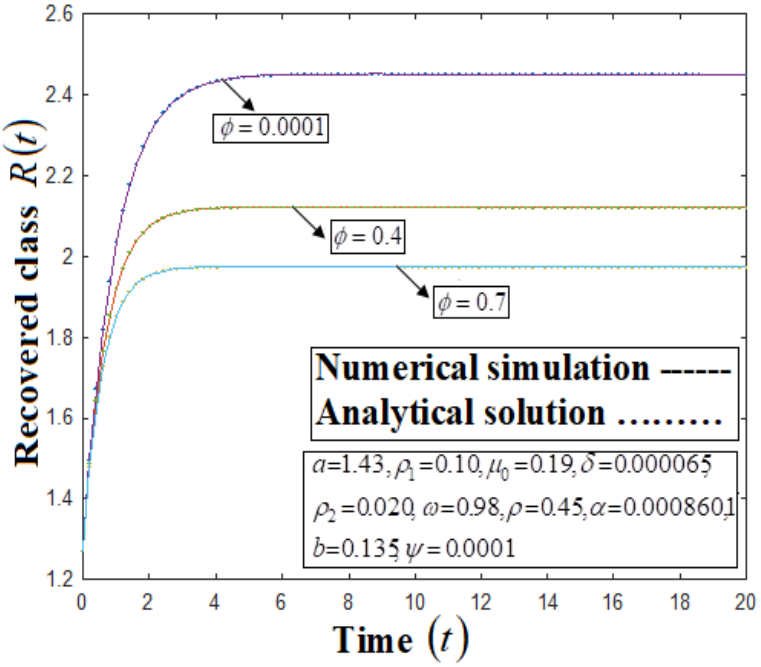

Figure 29. Effect of immunization and sick class contact ϕ in recovered $R(t)$.

6. Conclusion

To help eradicate COVID-19, it is recommended that governments prioritize widespread immunization for vulnerable populations. Additionally, hospitals should be equipped with advanced healthcare facilities and life-saving technologies to effectively treat infected individuals. To further curb the spread, adherence to public health measures such as curfews, isolation, and the consistent use of face masks is strongly advised. Using the HAM, the approximate analytical result of the COVID-19 models for the susceptible S, exposed E, vaccinated V, infected I and recovered R was obtained for all parameter values. To demonstrate the efficacy of the approach, graphical representations of each parameter in the model were shown. Our approximate analytical results corresponded nicely with the numerical simulation. To further expand the findings of this study, it would be worthwhile to extend the current model by incorporating quarantine, hospitalization, and awareness of COVID-19. Awareness plays a key role in encouraging individuals to get vaccinated and seek hospitalization when necessary. Therefore, examining the combined effects of awareness, quarantine, and hospitalization on controlling the COVID-19 outbreak would be of significant interest. The outcome causes the following:

• According to our research, if we increase the pace of recruitment a, we may quickly identify susceptible individuals $S(t)$ and lower the number of exposed individuals $E(t)$ by increasing the rate at which vaccination reduces infection α.

• Infected class $I(t)$ decreases by raising the recovery rate ψ at the infected population.

• To increase the recovered population $R(t)$, it is recommended that the recruitment rate into the vaccination class b be enhanced.

• Guidance on viral control is provided to support the community in overcoming the pandemic by prioritizing vaccination for individuals with weakened immune systems.

7. Appendices

MATLAB program to find the numerical simulation of Eqns. (2.1)-(2.5)

$functiongraphmain3$
$options = odeset('RelTol', 1e-6,'Stats','on');$
$Xo = [217.342565, 100, 1.386348, 1.1, 1.271087];$
$tspan = [0, 20]; ss$
tic
$[t, X] = ode45(@TestFunction, tspan, Xo, options);$
toc
$figure$
$holdon$
$plot(t, X(:, 1),'-')$
$plot(t, X(:, 2),'-')$
$plot(t, X(:, 3),'-')$
$plot(t, X(:, 4),'-')$
$plot(t, X(:, 5),'-')$
$legend('S','E','V','I','R')$
$ylabel('Population')$
$xlabel('Time')$
$return$
$function[dx_dt] = TestFunction(, x)$
$a = 1.43; rho1 = 0.10; mu0 = 0.19; delta = 0.000065; rho2 = 0.020; omega = 0.98; rho = 0.45; alpha = 0.0008601;$
$b = 0.135; phi = 0.0001; psi = 0.0001;$
$dx_dt(1) = a - ((delta + rho + rho1) * x(1));$
$dx_dt(2) = ((rho + rho1) * x(1)) - (delta * x(2)) - ((rho2) * (alpha) * x(2) * x(3));$
$dx_dt(3) = ((rho2) * (alpha) * x(2) * x(3)) - ((delta + mu0 + omega - b + phi) * x(3));$
$dx_dt(4) = (phi * x(3)) - ((mu0 + delta + psi) * x(4));$
$dx_dt(5) = (omega * x(3)) + (psi * x(4)) - (delta * x(5));$
$dx_dt = dx_dt';$
$return$

Conflict of interests

The authors declare that there is no conflict of interests.

Acknowledgement

The authors are thankful to Sri. S. Natanagopal, Secretary, The Madura College Board, Dr. J. Suresh, The Principal, The Madura College and Dr. C. Thangapandi,

Head of the Department of Mathematics, The Madura College, Madurai, Tamil Nadu, India for their constant support to our research work.

References

[1] H. Alsaud, M. O. Kulachi, A. Ahmad and M. Taimoor, *Investigation of SEIR model with vaccinated effects using sustainable fractional approach for low immune individuals*, AIMS Mathematics, (2024), 9(4), 10208–10234.

[2] A. Atangana, *Modelling the spread of COVID-19 with new fractal-fractional operators: can the lockdown save mankind before vaccination?* Chaos, Solitons and Fractals, (2020), 136, 109860.

[3] A. Atangana, *Mathematical model of survival of fractional calculus, critics and their impact: How singular is our world?* Advances in Difference Equations, 2021(1), 403.

[4] A. Atangana and S. İğret Araz, *Mathematical model of COVID-19 spread in Turkey and South Africa: theory, methods, and applications*, Advances in Difference Equations, 2020, 1–89.

[5] D. Baccega, P. Castagno, A. Fernández Anta and M. Sereno, *Enhancing COVID-19 forecasting precision through the integration of compartmental models, machine learning and variants*, Scientific Reports, (2024), 14(1), 19220.

[6] C. M. Batistela, D. P. Correa, Á. M. Bueno and J. R. C. Piqueira, *SIRSi compartmental model for COVID-19 pandemic with immunity loss. Chaos*, Solitons and Fractals, (2021), 142, 110388.

[7] S. Bera, S. Khajanchi and T. K. Kar, *Stochastic persistence, extinction and stationary distribution in HTLV-I infection model with CTL immune response*, Qualitative Theory of Dynamical Systems, (2024), 23(1), 265.

[8] S. Bera, S. Khajanchi and T. K. Roy, *Dynamics of an HTLV-I infection model with delayed CTLs immune response*, Applied Mathematics and Computation, (2022), 430, 127206.

[9] S. R. Chawla, S. Ahmad, A. Khan, W. Albalawi, K. S. Nisar and H. M. Ali, *Stability analysis and optimal control of a generalized SIR epidemic model with harmonic mean type of incidence and nonlinear recovery rates*, Alexandria Engineering Journal, (2024), 97, 44–60.

[10] D. K. Das, S. Khajanchi and T. K. Kar, *The impact of the media awareness and optimal strategy on the prevalence of tuberculosis*, Applied Mathematics and Computation, (2020), 366, 124732.

[11] Q. Deng, *Dynamics and development of the COVID-19 epidemic in the United States: a compartmental model enhanced with deep learning techniques*, Journal of Medical Internet Research, (2020), 22(8), e21173.

[12] A. Dwivedi, R. Keval and S. Khajanchi, *Modeling optimal vaccination strategy for dengue epidemic model: a case study of India*, Physica Scripta, (2022), 97(8), 085214.

[13] L. Ebiwareme, R. E. Akpodee, and R. I. Ndu, *An application of LADM-Pade approximation for the analytical solution of the SIR infectious Disease Model*, International Journal of Innovation Engineering and Science Research, 2022, 6(2).

[14] M. Farman, M. Azeem and M. O. Ahmad, *Analysis of COVID-19 epidemic model with sumudu transform*, AIMS Public Health, 2022, 9(2), 316.

[15] A. Gatto, G. Accarino, V. Aloisi, F. Immorlano, F. Donato and G. Aloisio, *Limits of compartmental models and new opportunities for machine learning: a case study to forecast the second wave of COVID-19 hospitalizations in Lombardy, Italy*, In Informatics, 2021, 8(3), 57.

[16] S. Ghosh, J. Mondal and S. Khajanchi, *Effect of media awareness in the spread of infectious diseases*, Journal of Applied Mathematics and Computing, (2025), 1–28.

[17] S. Hussain, E. N. Madi, H. Khan, H. Gulzar, S. Etemad, S. Rezapour and M. K. Kaabar, *On the stochastic modeling of COVID-19 under the environmental white noise*, Journal of Function Spaces, 2022, (1), 4320865.

[18] R. Kahn, I. Holmdahl, S. Reddy, J. Jernigan, M. J. Mina and R. B. Slayton, *Mathematical modeling to inform vaccination strategies and testing approaches for coronavirus disease 2019 (COVID-19) in nursing homes*, Clinical Infectious Diseases, 2022, 74(4), 597–603.

[19] S. Khajanchi, S. Bera and T. K. Kar, *An Optimal Control Problem for HTLV-I Infection Model*, Optimal Control Applications and Methods, (2024).

[20] S. Khajanchi, S. Bera and T. K. Roy, *Mathematical analysis of the global dynamics of a HTLV-I infection model, considering the role of cytotoxic T-lymphocytes*, Mathematics and Computers in Simulation, (2021), 180, 354–378.

[21] M. M. Khalsaraei, *An improvement on the positivity results for 2-stage explicit Runge-Kutta methods*, Journal of computational and applied mathematics, 2010, 235(1), 137–143.

[22] M. Khan, S. Farasat Saddiq, S. Khan, S. Islam and F. Ahmad, *Application of homotopy perturbation method to an SIR epidemic model*, Journal of Applied Environmental and Biological Sciences, 2014, 4, 49–54.

[23] A. P. Lemos-Paiao, C. J. Silva and D. F. Torres, *A new compartmental epidemiological model for COVID-19 with a case study of Portugal*, Ecological Complexity, 2020, 44, 100885.

[24] X. Li, V. Patel, L. Duan, J. Mikuliak, J. Basran and N. D. Osgood, *Real-time epidemiology and acute care need monitoring and forecasting for covid-19 via Bayesian sequential Monte Carlo-leveraged transmission models*, International Journal of Environmental Research and Public Health, 2024, 21(2).

[25] S. Liao, *An explicit analytic solution to the Thomas-Fermi equation*, Applied Mathematics and Computation, 2003, 144(2-3), 495–506.

[26] S. Liao, *On the homotopy analysis method for nonlinear problems*, Applied mathematics and computation, 2004, 147(2), 499–513.

[27] J. Mondal and S. Khajanchi, *Mathematical modeling and optimal intervention strategies of the COVID-19 outbreak*, Nonlinear dynamics, 2022, 109(1), 177–202.

[28] P. A. Naik, M. Farman, A. Zehra, K. S. Nisar and E. Hincal, *Analysis and modeling with fractal-fractional operator for an epidemic model with reference to COVID-19 modeling*, Partial Differential Equations in Applied Mathematics, (2024), 10, 100663.

[29] I. Nesteruk, *Statistics-based predictions of coronavirus epidemic spreading in mainland China*, 2020.

[30] K. S. Nisar, M. Farman, M. Abdel-Aty and J. Cao, *A review on epidemic models in sight of fractional calculus*, Alexandria Engineering Journal, (2023), 75, 81–113.

[31] K. S. Nisar, M. Farman, M. Abdel-Aty and C. Ravichandran, *A review of fractional order epidemic models for life sciences problems: Past, present and future*, Alexandria Engineering Journal, (2024), 95, 283–305.

[32] K. S. Nisar, M. Farman, K. Jamil, A. Akgul and S. Jamil, *Computational and stability analysis of Ebola virus epidemic model with piecewise hybrid fractional operator*, Plos one, (2024), 19(4), e0298620.

[33] A. Olivares and E. Staffetti, *Robust optimal control of compartmental models in epidemiology: Application to the COVID-19 pandemic*, Communications in Nonlinear Science and Numerical Simulation, 2022, 111, 106509.

[34] A. Rahman and M. A. Kuddus, *Modelling the transmission dynamics of COVID-19 in six high-burden countries*, BioMed Research International, 2021, (1), 5089184.

[35] S. B. Ramezani, A. Amirlatifi and S. Rahimi, *A novel compartmental model to capture the nonlinear trend of COVID-19*, Computers in Biology and Medicine, 2021, 134, 104421.

[36] N. P. Ratchagar and S. P. Subramanian, *Seir Model of Seasonal Epidemic Diseases using HAM*, Applications and Applied Mathematics: An International Journal (AAM),2015, 10(2), 30.

[37] S. Romano, A. Fierro and A. Liccardo, *Beyond the peak: A deterministic compartment model for exploring the Covid-19 evolution in Italy*, PloS one, 2020, 15(11), e0241951.

[38] M. U. Saleem, M. Farman, K. S. Nisar, A. Ahmad, Z. Munir and E. Hincal, *Investigation and application of a classical piecewise hybrid with a fractional derivative for the epidemic model: Dynamical transmission and modeling*, Plos one, (2024), 19(8), e0307732.

[39] B. Seethalakshmi, V. Ananthaswamy and S. Narmatha, *Application of new homotopy perturbation method in solving a simple predator prey model with rich dynamics*, Advances and Applications in Mathematical Sciences, 2022, 21 (4), 2015–2025.

[40] K. Shah, R. U. Din, W. Deebani, P. Kumam and Z. Shah, *On nonlinear classical and fractional order dynamical system addressing COVID-19*, Results in Physics, 2021, 24, 104069.

[41] P. K. Tiwari, R. K. Rai, S. Khajanchi, R. K. Gupta and A. K. Misra, *Dynamics of coronavirus pandemic: effects of community awareness and global information campaigns*, The European Physical Journal Plus, (2021), 136(10), 994.

[42] C. Xu, M. Farman, A. Hasan, A. Akgül, M. Zakarya, W. Albalawi and C. Park, *Lyapunov stability and wave analysis of Covid-19 omicron variant of real data with fractional operator*, Alexandria Engineering Journal, 2022, 61(12), 11787–11802.

[43] Y. Zelenkov and I. Reshettsov, *Analysis of the COVID-19 pandemic using a compartmental model with time-varying parameters fitted by a genetic algorithm*, Expert Systems with Applications, 2023, 224, 120034.

[44] P. Zhou, X. L. Yang, X. G. Wang, B. Hu, L. Zhang, W. Zhang and Z. L. Shi, *A pneumonia outbreak associated with a new coronavirus of probable bat origin*, Nature, (2020), 579(7798), 270–273.

[45] N. Zhu, D. Zhang, W. Wang, X. Li, B. Yang, J. Song and W. Tan, *A novel coronavirus from patients with pneumonia in China, 2019*, New England Journal of Medicine, (2020), 382(8), 727–733.